Low sidelobe limited diffraction beams in the nonlinear regime

Sverre Holm and Fabrice Prieur
Department of Informatics, University of Oslo, P.O. Box 1080, NO-0316 Oslo, Norway

(Received 11 January 2010; revised 28 June 2010; accepted 1 July 2010)

In linear propagation, sidelobe levels of Bessel limited diffraction beams are only about 8 dB down relative to the mainlobe. In the nonlinear regime, these beams will have a region near the source where the side-lobe level of the second harmonic is 16 dB down, but this region has usually been considered to be so small that it is of little practical interest. In this paper it is shown that when there are only 1 to 3 sidelobes in a finite aperture Bessel beam, the second harmonic field will have low sidelobes for distances up to half of the depth of field. This result is backed up by simulations. In a medium with absorption, previous theory has shown that the sidelobes of the Bessel beam will also be reduced but only for absorption that was too high to be of practical use. Simulations presented here show that for breast tissue, which only has about 10% of the absorption of previous criteria, one will still get sidelobes which are comparable to that of a rectangular aperture even when the sidelobes would be high in a non-absorbing medium.
 [DOI: 10.1121/1.3467761]

PACS number(s): 43.35.Yb, 43.25.Cb [ROC] Pages: 1015–1020

I. INTRODUCTION

Over the last two decades the Bessel beam solution to the wave equation has been investigated in the fields of optics[1] and acoustics.[2,3] It is different from other beams in that it does not diffract with depth. This ensures a uniform beamwidth with depth, at least out to a certain depth for finite aperture sources. Therefore it is usually called a limited diffraction beam.

The characteristics of this beam is that the field varies laterally with ρ as a Bessel function of order n, $J_n(\alpha'\rho)$ where ρ is the transverse coordinate, and α' the transverse wavenumber of the Bessel beam. There is a solution for each order, n, of the Bessel function, but since the $n=0$ beam has the best mainlobe to sidelobe ratio, we will only be concerned with that beam here. But even this beam is characterized by a sidelobe to mainlobe ratio which is relatively poor, with the first sidelobe only 7.9 dB below the mainlobe. This is one of the reasons why Bessel beams have seen little use in applications.

Some suggestions for dealing with this have been proposed. One way is to use multiple transmissions and subtraction of beams with different orders,[4] but it may give blurring when the targets are non stationary, and its result may have a dynamic range problem due to the subtraction of larger signals. Bowtie limited diffraction beams have also been proposed.[5] They require a full two-dimensional array for their generation and rely on cancellation of high sidelobes for the transmitter when they fall in regions with low receiver sidelobes and vice versa. Another way is to use weighting,[6] but the improvement is marginal especially for the nearest sidelobes. The hybrid array proposed by Hooi *et al.*[7] is a different approach in that it combines a central spherical part with an outer conical part with the purpose of making the depth of field longer while preserving the sidelobe level of the spherical beam.

Like most beams, the Bessel beam will change character when the propagation is nonlinear. Ding and Lu[8] and Du *et al.*[9] were the first to report this. Du *et al.* found that in the near field, the Bessel beam's second harmonic will behave as $J_0^2(\alpha'\rho)$. Thus the sidelobes will be half that of the fundamental beam, i.e., the first sidelobe will fall to -15.8 dB, while the beamwidth is constant with depth. Synnevåg and Holm also found reduced sidelobe levels in the near field in a simulation study for finite aperture sources.[10] Cunningham and Hamilton[11] showed that under certain conditions, absorption in the medium will extend the region where the beam is given by $J_0^2(\alpha'\rho)$. In that case, the low sidelobe level may make the Bessel beam more attractive for many purposes as the level of the first sidelobe is now between those of common sources like a rectangular transducer (-13.3 dB) and a piston source (-17.6 dB). The sidelobe fall-off rate is -6 dB/octave similar to that for a rectangular source, but not as good as the -9 dB/octave of the circular source.

Most of the papers cited above as well as later papers by Ding and Lu[12] deal with an infinite Bessel source. Many of the papers also seem to consider the far field result where the beam is proportional to $J_0(2\alpha'\rho)$ and thus has high sidelobes, to be more important than the near field result. This may be due to the examples studied which have usually turned out to have such a small near field region that it has not been so interesting or useful.

The purpose of this paper is to show that in some cases the low sidelobe $J_0^2(\alpha'\rho)$ beam from a finite source in the nonlinear regime exists over a considerable distance. This applies both to non-attenuating and attenuating media. The paper starts by reviewing the range over which the squared Bessel beam for a finite aperture in a non-attenuating medium exists and compares that to the depth of field for the primary Bessel beam of order 0. We then find that there is a subset of Bessel beams which generate low sidelobe beams over a major part of their useful range. The result is verified by simulations. Then we present a simulation study for the case of attenuation. We show through simulation that previous criteria for obtaining the squared low-sidelobe Bessel

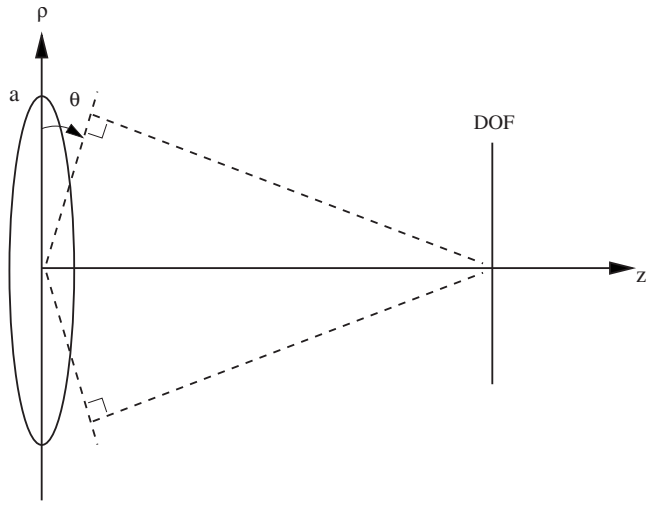

FIG. 1. Geometry showing the transducer of radius a and the depth of field.

beam are too conservative. This means that for practical media in e.g., medical ultrasound, low sidelobe second harmonic beams may exist over a large range, even if the low sidelobe solution does not exist in a non-attenuating media.

II. BESSEL BEAMS

For a plane circular source there is a single frequency solution to the wave equation where the pressure, P_1, varies with the radial dimension, ρ, as a Bessel function:[1]

$$P_1(\rho,z,t) = P_0 \cdot J_n(\alpha'\rho)e^{i(\beta' z-\omega_0 t)}. \tag{1}$$

Here t is the time, ω_0 is the angular frequency, and P_0 is the peak pressure at $z=0$. The beam propagates mainly in the z-direction perpendicular to ρ. The real parameters α' and β' are related to the wavenumber by:

$$\alpha'^2 + \beta'^2 = k^2. \tag{2}$$

For a finite source with radius a, we will use a normalized Bessel beam parameter $\alpha = a\alpha'$. Note that $\alpha=0$ gives the plane wave solution. The wavenumber is decomposed into β', which is the component along the z-axis and α', which is the component in the radial direction (ρ-direction). Therefore, the Bessel beam is composed of plane waves traveling at an angle to the z-axis given by:[1]

$$\sin\theta = \alpha'/k. \tag{3}$$

At a certain depth and with a finite aperture, the plane waves will no longer overlap. This results in a conical shadow zone which marks the end of the depth of field (DOF)[1] as shown in Fig. 1. The extent of the depth of field is from $z=0$ to

$$\mathrm{DOF}_{\mathrm{Bessel}} = a/\tan\theta \approx ka/\alpha' = ka^2/\alpha. \tag{4}$$

The Bessel beam is characterized by a beamwidth of:

$$\rho_C = C/\alpha' = C\frac{a}{\alpha}, \tag{5}$$

where C is a constant. For the -6 dB beamwidth $C=3.04$, and for the zero-to-zero beamwidth $C=4.81$.

One of the most popular examples of a Bessel beam to be investigated in the literature has a value for α of 30.02, i.e., it has a total of 10 lobes (1 mainlobe and 9 sidelobes).[3] However, Holm has shown that even low values for α such that the excitation only contains the mainlobe and a single sidelobe ($\alpha=5.52$) give close to uniform beamwidth within the depth of field.[13]

III. BESSEL BEAMS AND NONLINEAR PROPAGATION

A. Lossless propagation: Near and far field approximations

In nonlinear propagation, energy at the fundamental frequency will be transferred to harmonics. Ding and Lu[12] derived an expression for the second harmonic beam of an infinite n'th order Bessel source. These results will be applied here for $n=0$. Their derivation used a normalized axial coordinate $\eta \equiv z/z_0$, where $z_0 \equiv ka^2/2$ is the Rayleigh distance, and a normalized transversal coordinate $\xi \equiv \rho/a$, with a as the piston radius.

Under the assumptions that absorption and dispersion are negligible, and using the quasilinear solution of the Khokhlov-Zabolotskaya-Kuznetsov (KZK) equation,[14] Ding and Lu found that in a far field region characterized by

$$\alpha^2\eta \geq 4\pi, \tag{6}$$

the second harmonic of a Bessel beam can be approximated by:

$$\bar{q}_2(\xi,\eta) = -\frac{1-i}{4\pi^{1/2}\alpha}\eta^{1/2}J_0(2\alpha\xi)\exp\left(-\frac{i\alpha^2\eta}{2}\right), \tag{7}$$

where the pressure field of the second harmonic is $P_2 = \bar{q}_2 P_0$. This result is remarkable in that the beamwidth of the second harmonic, due to the dependence on $J_0(2\alpha\xi)$, is half that of the fundamental as pointed out by Ding and Lu. This is unlike most other beams and their harmonics. However, the sidelobes stay the same at the relatively high values of a Bessel function.

In the near field region the second harmonic beam can be approximated by:[12]

$$\bar{q}_2(\xi,\eta) = \frac{i\eta}{8}J_0^2(\alpha\xi)\exp\left(-\frac{i\alpha^2\eta}{2}\right). \tag{8}$$

The $J_0^2(\alpha\xi)$ term results in a beamwidth which is about 70% of that of the fundamental beam. It also gives reduced sidelobe levels. This makes the near field the more interesting part of the second harmonic beam to study here. A generalization of this result as well as that of Eq. (7) to a finite aperture, Gaussian weighted, Bessel beam was derived by Ding *et al.*,[15] but the sidelobe level of the beams in the two regions is more or less the same as given above for infinite apertures.

Ding and Lu[12] gave the extent of the near field region as $\alpha^2\eta \leq \pi$. Du *et al.*[9] were however the first to derive the near field result and gave the near field limit as

$$\alpha^2\eta \leq 4. \tag{9}$$

Later in the simulations, it will turn out that this limit is the more accurate one.

Cunningham and Hamilton[11] mention that the limits are proportional to the Rayleigh limit of a source with a radius normalized by the Bessel parameter, α. By manipulating the $\alpha^2\eta$ term an even more physical meaning appears. At the far field limit, and using Eq. (5), we get:

$$\alpha^2\eta = \frac{z}{z_0}\alpha^2 = z/\left(\frac{k(a/\alpha)^2}{2}\right) = C^2 z/\left(\frac{k\rho_C^2}{2}\right) = 4\pi. \tag{10}$$

If $C=2\sqrt{\pi}\approx 3.54$, the far field limit can be explained as the Rayleigh limit, $z=k\rho_C^2/2$, of a flat piston source with radius given by ρ_C, the mainlobe of the Bessel beam. Using Eq. (5) with $C\approx 3.54$, one can see that the definition of the mainlobe is then somewhere between the -6 dB width and the zero-to-zero width.

B. Lossless propagation: Condition for low sidelobes

In order to find the condition for the extent of the near field solution, one can combine the definition of the depth of field (DOF) for a finite source, Eq. (4), with the near and far field limits. This will result in a condition on α for placing the DOF between the limits, i.e.,

$$\alpha^2\eta = z\alpha^2/z_0|_{z=\mathrm{DOF}_{\mathrm{Bessel}}} = \frac{ka^2}{\alpha}\alpha^2/z_0 = 2\alpha. \tag{11}$$

Using the near-field limit of Eq. (9) this gives $\alpha=2$, and combination with the far-field limit of Eq. (6) gives $\alpha=2\pi \approx 6.28$.

The smallest value for α which can be used in practice is $\alpha=5.52$. This is the minimal Bessel beam investigated in Ref. 13. It will have all of its depth of field inside the region of the far field limit and should thus have relatively low sidelobes in a considerable part of the depth of field.

C. Effect of absorption

Cunningham and Hamilton[11] have extended the above result to a medium with absorption. The absorption is given by an absorption coefficient α_n at frequency $\omega=n\omega_0$ in Np/m which is normalized by the Rayleigh distance and by the Bessel parameter to $a_n=\alpha_n z_0/\alpha^2$. The result depends on the factor $\hat{a}=a_2-2a_1$. The usual case is that the absorption coefficient increases with frequency raised to a power, i.e., $\alpha_n = \alpha_0\omega^y = \alpha_0 n^y \omega_0^y$. This gives the absorption factor

$$\hat{a} = \alpha_0\omega_0^y(2^y-2)z_0/\alpha^2. \tag{12}$$

Thus this factor equals zero and the result becomes as in the lossless case either if $y=1$, i.e., with an absorption that increases linearly with frequency or in the obvious lossless case, when $\alpha_0=0$. As many different kinds of tissue can be modeled with y close to 1, this means that the second harmonic Bessel beam is often more or less the same in the lossless and lossy cases. This is also discussed in Ref. 16 and in the recent paper by Huang *et al.*[17]

If $\hat{a}$ is greater than unity the beam profile of the second harmonic can be approximated as being proportional to $J_0^2(\alpha\xi)$ in the far field, and away from minima of the Bessel profile. This phenomenon was given a physical explanation by Cunningham and Hamilton. They explain that the second harmonic can be seen as a superposition of the diffracting radiation from virtual source planes distant from the observation point, and the second harmonic components generated close to the observation point. The first contributors produce a $J_0(2\alpha\xi)$ beam profile, while the second produce a $J_0^2(\alpha\xi)$ beam profile. For large values of $\hat{a}$, a_2 is large in relation to a_1, hence the total field is dominated by the near field contribution generating the $J_0^2(\alpha\xi)$ profile. This case is interesting as it will extend the region with lower sidelobes to greater depths.

In the case of small values of $\hat{a}$ ($\hat{a}<10^{-2}$ was mentioned in Ref. 11), and far from the source, the near field contribution is almost as attenuated as the far field contribution, and the beam profile can be approximated as being proportional to $J_0(2\alpha\xi)$, as in the case of lossless propagation. This happens in a low-loss medium like water.

IV. RESULTS AND DISCUSSIONS

A. Method

Simulations were carried out using both our implementation of the angular spectrum method of Christopher and Parker[18,10] and the Bergen code.[19] The Christopher and Parker method takes care of nonlinear effects in the temporal frequency domain via a Fourier series solution to a lossless Burgers' equation. The Bergen code builds on the KZK equation,[20] and is therefore based on the same foundation as the derivation of the results in this paper. Pressure fields resulting from both types of simulation were found to be very similar. The KZK and Burgers' equations are valid under the same conditions of quasi linearity and for $ka\gg 1$.[21,22]

The Christopher and Parker method has two substeps. In the first it operates in the temporal frequency domain and handles nonlinear effects. In the second step, which operates in the angular spectrum domain, diffraction and absorption are taken care of for all harmonics. In this way a number of harmonics are propagated in the direction of propagation. The angular spectrum method was used for all simulations shown in this paper.

In order to obtain the pressure field at a depth z, following Christopher and Parker,[23] the radial extent of the simulation was set to $T=4\cdot a$, where a is the source radius. This is enough to avoid perturbation of the source replica in our case. The number of radial samples was set to $N=4T/\lambda$ where λ is the wavelength. The propagation step size in depth dz was set to 1 mm. The sound propagation speed, water density, and nonlinearity coefficient were set to $c=1500$ m/s, $\rho=1000$ kg/m^3, $\beta=3.5$ for water, and $\beta=5.82$ for breast tissue. The diffraction step was computed in the frequency domain using the ray theory-updated frequency sampled convolution (RFSC).[23] Attenuation is applied at each step for all harmonics using the formula

$$\bar{q}_n(m+1) = \bar{q}_n(m)\cdot 10^{-\alpha_0\cdot(n\cdot f_0/10^6)^y\cdot dz\cdot 100/20}, \tag{13}$$

where $\bar{q}_n(m)$ is the pressure of the nth harmonic at depth $m\cdot dz$, and α_0 is the attenuation coefficient in dB/MHz^y/cm.

The nonlinear substep is given by Christopher and Parker,[18] but since we work with the real amplitude or one-sided spectrum,[24] we have used twice the constant in the

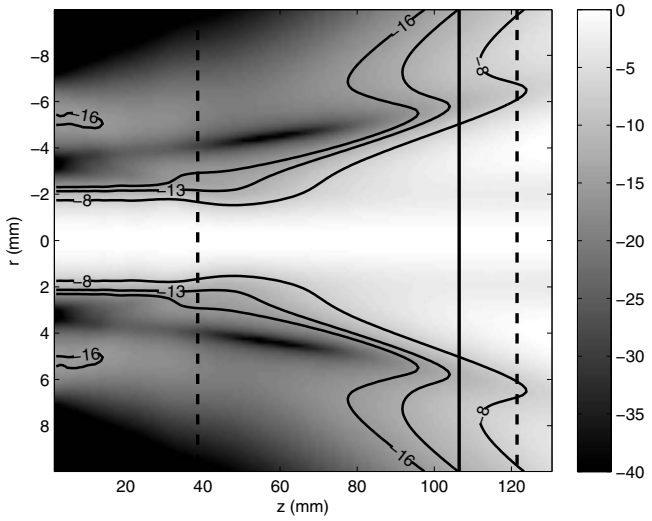

FIG. 2. Second harmonic pressure field −8 dB, −13 dB, and −16 dB contours with Bessel function apodization $J_0(\alpha\rho)$ in the case $\alpha=5.52$. The vertical lines show the depth of field (solid), and the near and far field limits (dashed), $a=7.5$ mm, $f=2.5$ MHz, $\beta=3.5$ (nonlinearity coefficient).

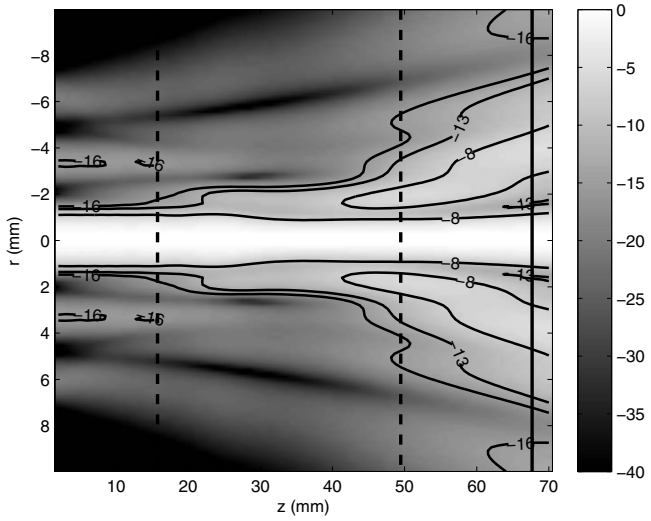

FIG. 3. Second harmonic pressure field −8 dB, −13 dB, and −16 dB contours with Bessel function apodization $J_0(\alpha\rho)$ in the case $\alpha=8.65$. The vertical lines show the depth of field (solid), and the near and far field limits (dashed), $a=7.5$ mm, $f=2.5$ MHz, $\beta=3.5$ (nonlinearity coefficient).

nonlinear substep [Eq. (3) in Ref. 18]. In all simulations using the angular spectrum method, 50 harmonics were used.

B. Sidelobes in the lossless case

In the first simulation, the maximum pressure field of a piston oscillating at 2.5 MHz, with an initial pressure $P_0=500$ kPa, is plotted up to a depth of 130 mm. The nonlinearity coefficient is set equal to that of water, $\beta=3.5$. The radius of the piston is $a=7.5$ mm, and its apodization is a Bessel function containing two lobes, i.e., $\alpha=5.52$. This value of α places the depth of field right inside the far field limit Eq. (6). Figure 2 shows the −8 dB, −13 dB, and −16 dB contours of the second harmonic pressure field. The dashed vertical lines show the near and far field limits, and the vertical solid line shows the depth of field.

Due to the low number of sidelobes in the Bessel excitation the Bessel beam is not fully developed into a limited diffraction beam. This can be seen from about 60 mm and out where the beam starts to split. Also extrapolating the shape of the sidelobes from the −8 dB contour at $z\simeq 70$ mm, the sudden widening of the −16 dB contour at $z\simeq 30$ mm will be interpreted as the appearance of the −16 dB level of the first sidelobes, and not as a widening of the main lobe.

The second simulation is done with the same piston at the same conditions except for the apodization that has been changed to a Bessel beam function containing three lobes, i.e., $\alpha=8.65$. This value of α places the depth of field just outside the far field limit defined in Eq. (11). It violates the condition that the depth of field should be between the near field and the far field limits, but in order to get an exact number of lobes on the radius of the aperture, the first available value for α above 5.52 is 8.65. Figure 3 shows the same contours of the second harmonic up to a depth of 70 mm. The vertical lines show the depth of field, and the near and far field limits as described previously.

The third simulation is done with the same piston and with apodization using a Bessel beam containing four lobes, i.e., $\alpha=11.8$. Figure 4 shows the −8 dB, and −16 dB contours as described before, up to a depth of 55 mm.

Finally Fig. 5 shows the −8 dB, and −16 dB levels of the pressure field for a piston of radius $a=25$ mm, oscillating at 2.5 MHz in a lossless medium, and with an initial pressure of $P_0=500$ kPa, which corresponds to a truncation of a Bessel beam after ten lobes, i.e., $\alpha=30.02$.

Table I sums up the near field and far field limits, and depth of field values [Eqs. (9), (6), and (4)]. Table II shows the depths at which the sidelobes reach −8, −13, −16 dB for the three values of α as well as the value for $\alpha^2\eta$ where the −8 and −16 dB levels are reached. These values should be compared to the near and far-field limits of Eqs. (9) and (6).

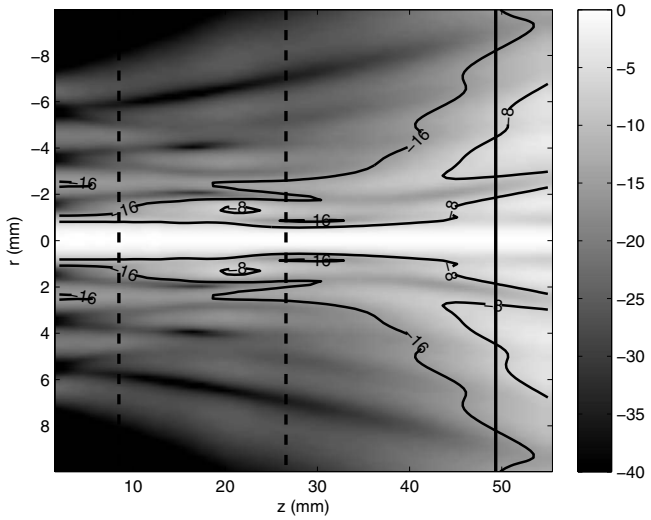

FIG. 4. Second harmonic pressure field −8 dB, and −16 dB contours with Bessel function apodization $J_0(\alpha\rho)$ in the case $\alpha=11.8$. The vertical lines show the depth of field (solid), and the near and far field limits (dashed), $a=7.5$ mm, $f=2.5$ MHz, $\beta=3.5$ (nonlinearity coefficient).

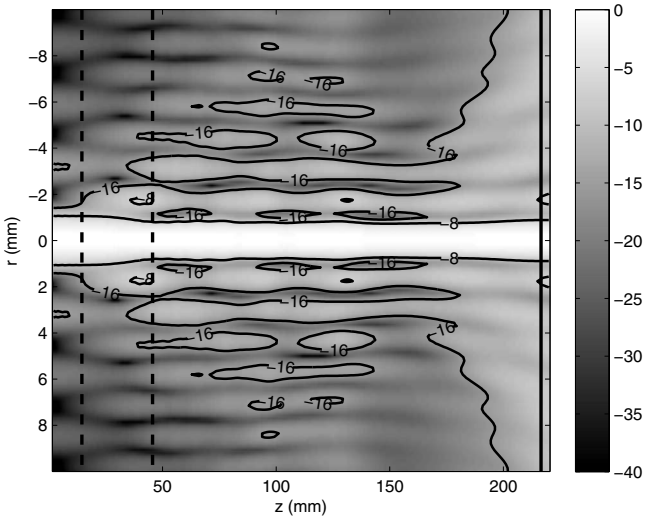

FIG. 5. Second harmonic pressure field −8 dB, and −16 dB contours with no absorption. The vertical lines show the depth of field (solid), and the near and far field limits (dashed), a=25 mm, f=2.5 MHz, α=30.02, β=3.5 (nonlinearity coefficient).

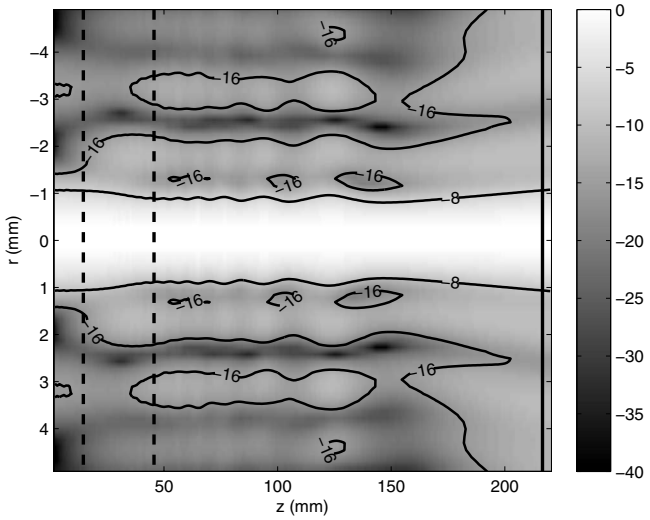

FIG. 6. Second harmonic pressure field −8 dB, and −16 dB contours with absorption coefficient of 0.75 dB/MHz$^{1.5}$/cm as in breast tissue. Vertical solid line shows depth of field, dashed lines show near and far field limits. a=25 mm, f=2.5 MHz, α=30.02, β=5.82.

From Figs. 2–4 and Table II it is clear that the sidelobes appear later in the useful field region for smaller values of α, and that up to half of the useful range (DOF) has sidelobes which are similar to those of a rectangular source or better (<−13 dB). One can also see that the sidelobes stay below this value to approximately twice the near field distance. This sidelobe level represents a significant improvement compared to a Bessel beam in linear propagation.

Concerning the validity of near and far field limits, it appears that the near field limit from Ding *et al.*[12] is a little conservative and that often the main lobe follows a $J_0^2(\alpha\xi)$ beam profile with low sidelobe levels deeper in the field. In Table II one can see that this occurs out to a distance which is close to the near field limit of Eq. (9) except for the smallest value of α.

The far field limit of Eq. (6) is very close to the depth at which the main lobe has narrowed down to the width of the $J_0(2\alpha\xi)$ beam profile, but the higher sidelobes occur inside this limit at a value of $\alpha^2\eta$ closer to 3π than 4π. Between the near and far-field limits there is a gradual build-up of sidelobes and at the same time a narrowing of the mainlobe.

TABLE I. Pressure field limit for varying Bessel parameter. α: Bessel parameter, a: piston radius, NF: Near field limit, FF: Far field limit, DOF: Depth of field.

α	a (mm)	NF (mm)	FF (mm)	DOF (mm)
5.52	7.5	38.7	121.5	106.4
8.65	7.5	15.8	49.5	67.7
11.8	7.5	8.4	26.6	49.4
30.02	25	14.5	45.6	216.6

TABLE II. Depths for specific sidelobe levels and derived values.

α	$z\|_{-16\text{ dB}}$ (mm)	$z\|_{-13\text{ dB}}$ (mm)	$z\|_{-8\text{ dB}}$ (mm)	$\alpha^2\eta\|_{-16\text{ dB}}$	$\alpha^2\eta\|_{-8\text{ dB}}$	$\frac{z\|_{-13\text{ dB}}}{\text{DOF}}$ (%)
5.52	31	53	70	3.20	2.31π	49.8
8.65	16	21.4	41	4.05	3.32π	31.6
11.8	8.5	11.5	18.4	4.02	2.77π	23.3
30.02	15	20.5	35	4.12	3.07π	9.5

C. Influence of absorption

In all the remaining simulations, α=30.02 and should be compared to the lossless case in Fig. 5. For confirmation, we simulated the case of an absorption coefficient which is proportional to frequency (y=1), as in muscle tissue, but the result is indistinguishable from the lossless case as expected.

The absorption was then set to simulate an absorption in breast tissue. Various values for the absorption parameters are given for this case, but according to Table IV.16 in Ref. 25, the frequency exponent dependency is y=1.5, resulting in a large positive value for $\hat{a}$. Figure 6 shows the −8 dB, and −16 dB levels of the pressure field with an absorption coefficient of 0.75 dB/MHz$^{1.5}$/cm. The value of the nonlinearity coefficient was β=5.82 (taken from Table IV.11 in Ref. 25), and no dispersion was accounted for.

Table III shows the medium parameters for the three above cases. Values for muscle and breast are taken from Table B.1 in Ref. 26, and Table 4.16 in Ref. 25 respectively.

Figure 6 shows that sidelobes usually are slightly higher than −16 dB for shallow depths, and stay at this level for $z \leq 155$ mm. The sidelobe level never comes close to −8 dB. On the other hand we get a sidelobe level comparable to

TABLE III. Medium parameters. α_0 is absorption given in dB/MHz^y/cm, β is nonlinearity coefficient, and $\hat{a}$ is given by Eq. (12).

Medium	α_0 (dB/MHz^y/cm)	y	β	$\hat{a}$ (Np)
Water	2×10^{-3}	2	3.5	0.001
Muscle	0.57	1	4.72	0
Breast	0.75	1.5	5.82	0.10

that of a rectangular array (−13 dB) over most of the simulated range. Thus the sidelobes are greatly reduced compared to a Bessel beam in the linear regime. Even if $\hat{a}$ does not satisfy the high absorption limit defined by Cunningham and Hamilton[11] ($\hat{a} \gtrsim 1$), the pressure field simulated in Fig. 6 shows that $\hat{a} \approx 0.1$ is enough for the sidelobe level to reach an acceptable value.

V. CONCLUSION

The purpose of this paper has been to demonstrate that limited diffraction Bessel beams which only have sidelobes in the 7–8 dB range, can show improved sidelobe levels for the second-harmonic beam in the nonlinear regime.

We have shown that when the number of lobes in a finite aperture Bessel beam is small (i.e., only 1–3 sidelobes), the second harmonic field will have low sidelobes over a considerable part of the depth of field. In this case, the beam is proportional to a squared Bessel beam with sidelobes in the 15–16 dB range. The extent of this region has been derived by comparing the depth of field of finite aperture Bessel beams with the criteria for low and high sidelobe regions of the second harmonic field. This result has been backed up by simulations. Previously, this part of the field has usually been dismissed since most papers only consider relatively high values of the Bessel beam parameters where this part of the field is very small.

Another way to obtain low sidelobes is to excite a Bessel beam in the nonlinear regime with high absorption which deviates much from linear frequency dependency. However the criterion for getting low sidelobes derived by Cunningham and Hamilton[11] dictates such a high absorption that it in practise excludes ultrasound propagation in tissue. Through simulation we have shown that for breast tissue, which only has about 10% of the absorption of this criterion, one will still get sidelobes which are comparable to that of rectangular apertures.

ACKNOWLEDGMENTS

We would like to thank Dr. Andreas Austeng for his help with the development of the simulator and Dr. Peter Näsholm and the associate editor for helpful comments. This research was partly financed by the Norwegian Research Council in the project "High resolution imaging and beamforming."

[1]J. Durnin, "Exact solutions for nondiffracting beams. I. The scalar theory," J. Opt. Soc. Am. A **4**, 651–654 (1987).
[2]D. Hsu, F. Margetan, and D. Thompson, "Bessel beam ultrasonic transducer: Fabrication method and experimental results," Appl. Phys. Lett. **55**, 2066–2068 (1989).
[3]J.-Y. Lu and J. F. Greenleaf, "Ultrasonic nondiffracting transducer for medical imaging," IEEE Trans. Ultrason. Ferroelectr. Freq. Control **37**, 438–447 (1990).
[4]J.-Y. Lu and J. F. Greenleaf, "Sidelobe reduction for limited diffraction pulse-echo systems," IEEE Trans. Ultrason. Ferroelectr. Freq. Control **40**, 735–746 (1993).
[5]J.-Y. Lu, "Bowtie limited diffraction beams for low-sidelobe and large depth of field imaging," IEEE Trans. Ultrason. Ferroelectr. Freq. Control **42**, 1050–1063 (1995).
[6]S. He and J.-Y. Lu, "Sidelobe reduction of limited diffraction beams with Chebyshev aperture apodization," J. Acoust. Soc. Am. **107**, 3556–3559 (2000).
[7]F.Hooi, K. E. Thomenius, R. Fisher, and P. L. Carson, "Hybrid beamforming and steering with reconfigurable arrays," IEEE Trans. Ultrason. Ferroelectr. Freq. Control **57**, 1311–1319 (2010).
[8]D. Ding and Z. Lu, "The second harmonic component in the Bessel beam," Appl. Phys. Lett. **68**, 608–610 (1996).
[9]G. Du, Y. Zhang, and Z. Zhu, "Nonlinear distortion of a non-diffraction ultrasonic field," in Proceedings of the 14th International Symposium on Nonlinear Acoustics (1996), pp. 189–193.
[10]J.-F. Synnevåg and S. Holm, "Non-linear propagation of limited diffraction beams," in Proceedings of the IEEE Ultrasonics Symposium, Sendai, Japan (1998), pp. 1885–1888.
[11]K. N. Cunningham and M. F. Hamilton, "Bessel beams of finite amplitude in absorbing fluids," J. Acoust. Soc. Am. **108**, 519–525 (2000).
[12]D. Ding and J.-Y. Lu, "Second-harmonic generation of the nth-order Bessel beam," Phys. Rev. E **61**, 2038–2041 (2000).
[13]S. Holm, "Bessel and conical beams and approximation with annular arrays," IEEE Trans. Ultrason. Ferroelectr. Freq. Control **45**, 712–718 (1998).
[14]S. Aanonsen, T. Barkve, J. Tjøtta, and S. Tjøtta, "Distortion and harmonic generation in the nearfield of a finite amplitude sound beam," J. Acoust. Soc. Am. **75**, 749–768 (1984).
[15]D.-S. Ding, S. Wang, and Y. Wang, "Nonlinear propagation of Bessel–Gauss ultrasonic beams," J. Appl. Phys. **86**, 1716–1723 (1999).
[16]D.-S. Ding, J.-Y. Xu, and Y.-J. Wang, "Second-harmonic generation of Bessel beams in lossy media," Chin. Phys. Lett. **19**, 689–690 (2002).
[17]J. Huang, D. Ding, and Y. Hsu, "Second-harmonic generation of practical Bessel beams," J. Sound Vib. **328**, 148–155 (2009).
[18]P. T. Christopher and K. J. Parker, "New approaches to nonlinear diffractive field propagation," J. Acoust. Soc. Am. **90**, 488–499 (1991).
[19]J. Berntsen, http://folk.uib.no/nmajb/Bergencode.html (Last viewed 1/11/2010).
[20]J. Berntsen, "Numerical calculations of finite amplitude sound beams," *Frontiers of Nonlinear Acoustics*, in Proceedings of the 12th ISNA, edited by M. F. Hamilton and D. T. Blackstock (Elsevier, New York, 1990), pp. 191–196.
[21]"Model equations," in *Nonlinear Acoustics*, edited by M. F. Hamilton and D. T. Blackstock (Academic, Boston, 1998), Chap. 3, pp. 56–63.
[22]J. N. Tjøtta and S. Tjøtta, "Nonlinear equations of acoustics, with application to parametric acoustic arrays," J. Acoust. Soc. Am. **69**, 1644–1652 (1981).
[23]P. T. Christopher and K. J. Parker, "New approaches to the linear propagation of acoustic fields," J. Acoust. Soc. Am. **90**, 507–521 (1991).
[24]D. H. Trivett and A. L. Van Buren, "Comments on "Distortion of finite amplitude ultrasound in lossy media," by M. E. Haran and B. D. Cook [J. Acoust. Soc. Am. 73, 774–779 (1983)]," J. Acoust. Soc. Am. **76**, 1257–1258 (1984).
[25]F. A. Duck, "Acoustic properties of tissue at ultrasonic frequencies," *Physical Properties of Tissues—A Comprehensive Reference Book* (Academic, San Diego, 1990), Chap. 4, pp. 98–108.
[26]T. L. Szabo, *Diagnostic Ultrasound Imaging: Inside Out* (Elsevier, Amsterdam, 2004), p. 535.